Kernel-Specific Gaussian Process for Predicting Pipe Wall Thickness Maps

Lei Shi, Liye Sun, Teresa Vidal-Calleja, Jaime Valls Miro
Centre for Autonomous Systems,
Faculty of Engineering and Information Technology
University of Technology Sydney, Australia
{ Lei.Shi-1 | Teresa.VidalCalleja | Jaime.VallsMiro }@uts.edu.au, Liye.Sun@student.uts.edu.au

Abstract

Data organised in 2.5D such as elevation and thickness maps has been extensively studied in the fields of robotics and geostatistics. These maps are typically a probabilistic 2D grid that stores an estimated value (height or thickness) for each cell. Modelling the spatial dependencies and making inference on new grid locations is a common task that has been addressed using Gaussian random fields. However, inference faraway from the training areas results quite uncertain, therefore not informative enough for some applications. The objective of this research is to model the status of a pipeline based on limited and sparse local assessments, predicting the likely condition on pipes that have not been inspected. A customised kernel for Gaussian Processes (GP) is proposed to capture the spatial correlation of the pipe wall thickness data. An estimate of the likely condition of non-inspected pipes is achieved by concretising GP to a multivariate Gaussian distribution and generating realisations from the distribution. The performance of this approach is evaluated on various thickness maps from the same pipeline, where data have been obtained by measuring the actual remaining wall thickness. The output of this work aims to serve as the input of a structural analysis for failure risk estimation.

Keywords : Gaussian Process, Kernels, Mapping.

1 Introduction

The water industry usually owns and maintains a large volume of buried assets such as pipelines. The prediction of a pipe's remaining life is important when developing effective renewal programs and reducing the incidence of catastrophic failures [Ulapane *et al.*, 2014], [Miro *et al.*, 2013]. In order to achieve this objective, a better understanding of the current condition of buried pipes relying on Non-destructive testing (NDT) technologies plays an influential role. Although there have been some efforts investigating the complicated mechanism of corrosion in a temporal context considering the environmental factors, there is still an absence of an extensively validated model [Petersen *et al.*, 2014] [Bonds *et al.*, 2005]. A common practice in conducting NDT on buried pipelines involves exposing one or several pipe segments, assessing the condition of these samples, summarising the extreme measurements such as pitting or minimum remaining wall thickness, and extrapolating local inspection data into uninspected regions using Extreme Value Analysis (EVA) [Schneider, 2009]. Further prediction on the probability of future failure can be conducted on the extrapolation results via statistical tools or structural reliability analysis [Schneider, 2009] [Rajeev *et al.*, 2014] [Li and Mahmoodian, 2013]. The extrapolation procedure is a data-driven approach which does not require full understanding of the corrosion behaviour.

The potential of condition assessment is not fully exploited by analysing only extreme values on the NDT measurements. Local NDT inspections provide measurements commonly in the form of 2.5-dimensional (2.5D) data, where axial and circumferential locations are associate to wall thickness of the pipe. Modelling the spatial correlation in these local assessments can potentially improve prediction by using the rich information contained in the measurements. For example, realisations of an uninspected area as wall thickness maps at the same resolution of the local inspection outcome are supposed to be more suitable for consequent structural analysis using Monte Carlo simulation [Spanos and Zeldin, 1998] or other conventional approaches.

Modelling spatial dependencies for 2.5D data has been largely studied in the past. Mathematically the problem can be described as a random field which is a collection of random variables of the form $\{y_{\mathbf{x}}, \mathbf{x} \in \mathbf{R}^d\}$, where $y_{\mathbf{x}}$ is the quantity measured at the position $\mathbf{x}$ [Lord *et al.*, 2014]. Random fields are also known as spatial processes

that are defined for spatially arranged measurements and patterns modelling for instance, univariate [Kroese and Botev, 2013] or multivariate [Schlather *et al.*, 2015] processes. Random fields can be statistically specified by its mean and covariance [Lord *et al.*, 2014] [Kroese and Botev, 2013]. When the mean is constant, depending on the covariances there are stationary random fields whose covariances are invariant under translations [Kroese and Botev, 2013], isotropic stationary random fields whose covariances are invariant under both translations and rotations [Kroese and Botev, 2013], and anisotropic stationary random fields whose covariances are directionally dependent [Lord *et al.*, 2014]. Furthermore, a more specific type of random field being studied extensively is Gaussian Random Fields [Davies and Bryant, 2013], also known as Gaussian Spatial Processes [Kroese and Botev, 2013] or Gaussian Process (GP) [Bishop, 2006] [Rasmussen and Williams, 2006]. In this case the random variables of a random field jointly have a multivariate normal distribution [Kroese and Botev, 2013].

In robotics, Gaussian Processes have been employed in terrain and surface modelling [O'Callaghan and Ramos, 2012] [Smith *et al.*, 2010] [Vasudevan *et al.*, 2009] [Kersting *et al.*, 2007]. In all these works, the utilisation varies with the properties of the applications, the structure of the model and usage of the correlation information. The use of these probabilistic tools for thickness mapping has recently been tackled by the authors for an application on pipeline condition assessment [Sun *et al.*, 2015][Vidal-Calleja *et al.*, 2014]. In our previous study, the spatial correlation of the profile is learnt by using a Gaussian Process model to produce a prior map for the fusion purposes. This model has been studied further in this current work to incorporate pipe's characteristics into the knowledge of the covariance function. We also propose the use of Gaussian Process realisations instead of inference, as it results in a more suitable interpretation of the condition of the pipe in uninspected areas, in particular, when these areas are faraway from the training data. Moreover, in the case that the global location information of the target area is missing, inference becomes impossible and realisation would be the only way of predicting the condition of the area of interest.

In summary, the contribution of this research work is two-fold: 1) a design of the kernel for modelling spatial correlation in pipes and 2) the use of realisations as opposed to Gaussian Process inference to extrapolate the conditions of the same pipe cohort together with the analysis of the prediction performance using different metrics. The rest of this paper is arranged as follows. Section 2 discusses the underlying approach of modelling the spatial data using Gaussian Processes and the design of a composite covariance function considering the properties of the target to be modelled. The experimental setup including data sets and evaluation metrics is described in Section 3. Corresponding experimental results are presented in Section 4 with analysis and discussion. Section 5 concludes the paper. In the context of this paper, we use the two terms kernel and covariance function interchangeably.

2 Approach

This section provides the detailed methodology for modelling spatially correlated data using Gaussian Processes in the application of pipe wall thickness mapping, and generating realisations from the learned model. GPs will be introduced in the aspects of problem identification, probabilistic modelling, parameter estimation, inference and realisation. This is followed by a comprehensive and application-specific discussion on kernel design.

2.1 Gaussian Processes

Gaussian Processes define the probability distribution over functions, any finite number of which have consistent joint Gaussian distribution.

Consider n thickness-location pairs $\mathcal{D} = \{(y_1, \mathbf{x}_1), (y_2, \mathbf{x}_2), ..., (y_n, \mathbf{x}_n)\}$, where $\mathbf{x}_i \in X$ is the position in $\mathbf{R}^d$ from which the thickness measurements $y_i \in Y$ was taken. The data set $\mathcal{D}$ is assumed to be drawn from a noisy process

$$y_i = f(\mathbf{x}_i) + \epsilon_i, \text{ where } \epsilon_i \sim \mathcal{N}(0, \sigma_n^2) \tag{1}$$

where noise ϵ_i follows independent, identically distributed zero-mean Gaussian with variance σ_n^2. Gaussian Processes are used to learn the distribution $p(\boldsymbol{f}|X, \mathcal{D})$ from $\mathcal{D}$ and have the capability of inferring $p(\boldsymbol{f}|X^*, \mathcal{D})$ for arbitrary location X^*.

Having specified the mean and covariance functions and identified the hyper-parameter set $\boldsymbol{\theta}$, parameter estimation can be conducted through optimisation by maximizing the likelihood function as described in equation 2.

$$\begin{aligned} \log p(\mathbf{y}|X) = &-\frac{1}{2}(\mathbf{y} - \boldsymbol{m}(X))^\top K_y^{-1}(\mathbf{y} - \boldsymbol{m}(X)) \\ &-\frac{1}{2}\log|K_y| - \frac{n}{2}\log 2\pi \end{aligned} \tag{2}$$

where $K_y = K(X, X) + \sigma_n^2 I$ denotes the joint prior distribution covariance of the function at positions X. The variance of the noise σ_n^2 is another parameter to be learned together with $\boldsymbol{\theta}$. Standard gradient descent can be used in parameter estimation [Rasmussen and Williams, 2006].

Inference at a finite set of query locations X^* can be performed by calculating the predicted mean $\boldsymbol{\mu}$ and covariance P.

$$\boldsymbol{\mu} = \boldsymbol{m}(X^*) + K(X^*, X)K_y^{-1}(\mathbf{y} - \boldsymbol{m}(X)) \tag{3}$$

$$P = K(X^*, X^*) - K(X^*, X)K_y^{-1}K(X^*, X)^\top \tag{4}$$

The matrix $K(X^*, X)$ is obtained from the covariance function K and it indicates the cross correlation between the function at the prediction points X^* and the training inputs X.

2.2 Realisations of Gaussian Processes

As the test data itself at query locations X^* follows the Multivariate Gaussian Distribution $\mathcal{N}(\boldsymbol{m}(X^*), K(X^*, X^*) + \sigma_n^2 I)$, wherever inference cannot be done the learned model can still be simulated. There are various methods of generating realisations of a Gaussian Process, which is also known as simulation or sampling. Cholesky decomposition is one of the conventional approaches although it has its limitation on large scale implementation [Kroese and Botev, 2013] [Schlather *et al.*, 2015]. Circular embedding is an alternative technique to efficiently simulate a Gaussian Process [Schlather *et al.*, 2015] [Davies and Bryant, 2013]. In our application, the maximum scale of data we are currently dealing with is about $10^3 \times 10^3$, which is possible for Cholesky decomposition to handle. For future work of processing higher resolution data or longer pipe segments we may need to turn to Circular embedding or some other algorithms.

2.3 Kernel Design

Gaussian Processes are completely specified by the mean function m and covariance function K. The mean function is usually set to be zero via normalization or can also be chosen explicitly. The covariance function controls the smoothness property of the processes, and the parameters of covariance function govern the effective range of correlation and the variability of the process. In this application we consider const-mean process, all that is needed to characterise the Gaussian Processes is the covariance function.

In our previous work targeting at data fusion, we have gone through an extensive model selection on most common covariance functions and chosen an isotropic Matérn family covariance function as shown in equation 5 [Rasmussen and Nickisch, 2010], because the fusion outcomes showed best results with it.

$$K(X, X^*) = \sigma_1^2 \left(1 + \sqrt{\frac{3\left(d_a^2 + d_c^2\right)}{l_1^2}}\right) \exp\left(-\sqrt{\frac{3\left(d_a^2 + d_c^2\right)}{l_1^2}}\right) \tag{5}$$

where d_a and d_c are absolute values of the axial and circumferential distances respectively. The length-scale l_1 and the variance σ_1 constitute the hyper-parameter set $\boldsymbol{\theta}$. Despite of its simplicity, the fact that this covariance function does not consider the 2π-periodic property in the circumferential direction becomes a theoretical weakness in this particular application.

There is no single covariance function that fits all modelling tasks. Depending on the purpose at hand, modified or composite covariance functions allow more flexibility in the model. The usage of prior knowledge in choosing appropriate covariance functions is also encouraged [Tesch *et al.*, 2011]. The effectiveness of using periodic covariance function in the study of seasonal variation and physical phenomena has been discussed in literature [Rasmussen and Williams, 2006] [Tartakovsky and Xiu, 2006]. In modelling the wall thickness of buried pipes we first of all consider the anisotropic properties. Different circumferential locations on a buried pipe usually imply different depth underground, while different axial locations generally stay at the save depth. Therefore the pipe surface condition can be considered as anisotropic. Furthermore, given the cylinder shape of pipes, the distance in the circumferential direction is known to be 2π-periodic. The last assumption is that the influence in either direction conjunctionally affects the other direction. Therefore the covariance functions for each direction needs to be multiplied. Under these facts and assumptions we propose a basic covariance function composition as the product of a periodical covariance function for the circumferential direction and a non-periodical covariance function for the axial direction. To take this one step further, we believe that different basic covariance function compositions have different manners of capturing the spatial correlation patterns so a linear combination of multiple basic compositions will have more flexibility and advantages. In the meantime the number of free parameters in the covariance function should be restricted to avoid overfitting.

The propose anisotropic composite covariance function, mathematically described in equation 6, is a linear combination of two basic compositions. The first one is the product of a periodic covariance function and a Matérn family covariance function for circumferential and axial distances respectively, the second one is the product of a periodic covariance function and a rational quadratic covariance function for circumferential and axial distances respectively. There are seven free parameters is the proposed covariance function. Please note that it has been theoretically proved that the sum of two kernels is a kernel and the product of two kernels is also a kernel [Rasmussen and Williams, 2006]. Therefore the proposed covariance function is guaranteed to be positive semidefinite.

$$K(X, X^*) = \sigma_1^2\sigma_2^2 \exp\left(-\frac{2}{l_1^2}\sin^2\left(\frac{\pi d_c}{p}\right) - \frac{d_a}{l_2}\right) + \sigma_3^2\sigma_4^2 \exp\left(-\frac{2}{l_3^2}\sin^2\left(\frac{\pi d_c}{p}\right)\right)\left(1 + \frac{d_a}{2\alpha l_4^2}\right)^{-\alpha} \tag{6}$$

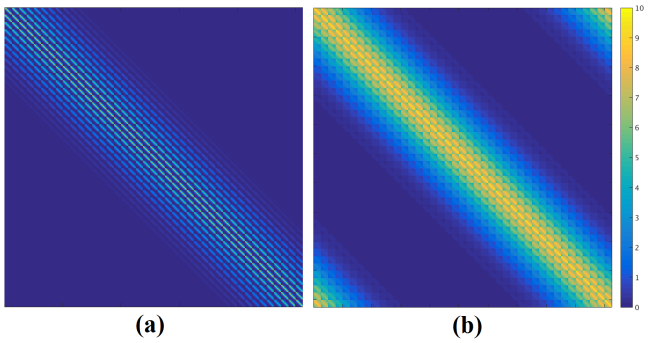

Figure 1: Covariance matrices generated from a) the isotropic Matern family covariance function, b) the proposed composite anisotropic covariance function

where d_a and d_c are absolute values of axial and circumferential distances respectively. σ_2 and σ_4 are clamped to one as a measure to avoid equivalent solutions. p is clamped to a constant according to the target pipe diameter and sensor resolution so that the distance in the circumferential direction is guaranteed to be 2π-periodic.

A visual comparison of covariance matrices generated from the above two covariance functions is presented in Figure 1. It can be visually verified that the covariance matrix generated from the proposed composite anisotropic covariance function has more expanded correlation.

The correlation coefficient plots in Figure 2 partially demonstrate the correctness of the assumptions for the proposed composite anisotropic covariance function. Statistics on the ground-truth data shows that for any given spot on the pipe, the thickness correlation is anisotropic. The proposed covariance function is able to effectively capture the actual correlation, especially the significant region of the correlation.

3 Experimental Setup

3.1 Data Set

The evaluation is performed on 12 pipe segments of about 1 meter long each. These samples are taken from a decommissioned 1.5 km long section of 600mm diameter cement lined cast iron pipe at Strathfield, Sydney [Miro *et al.*, 2013]. Pipe wall thickness profiles at sub-millimeter spatial resolution are produced through high-resolution geometric 3D laser scans of both outer and inner surfaces of the exhumed and grit-blasted pipes together with algorithms to extract the thickness information out of the 3D geometric models [Miro *et al.*, 2013] [Skinner *et al.*, 2014]. Each of the 12 pipe segments is assigned an ID from S1 to S12 which does not necessarily imply a spatial order. An illustrative example of the pipe wall thickness map production procedure can be found in Figure 3.

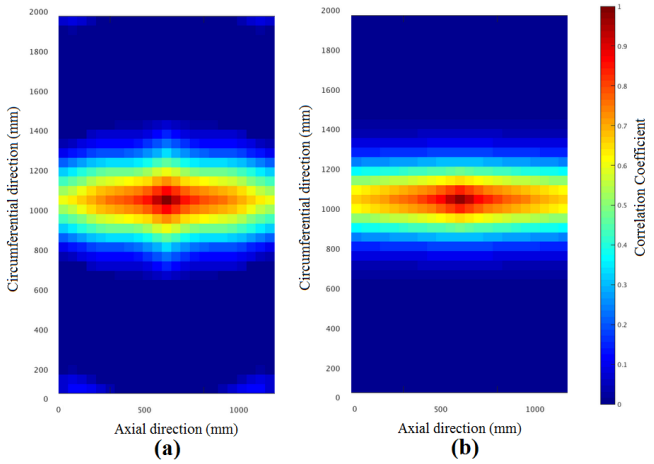

Figure 2: Typical correlation coefficient plot(s) for remaining wall thickness w.r.t the spot at the centre of the plot(s), generated from a) the ground-truth data, b) the proposed composite anisotropic covariance function

In order to reflect the real-world situation the ground-truth data is averaged out at the spatial resolution of 5 cm by 5 cm to mimic the output of an external NDT sensor [Ulapane *et al.*, 2014]. Local inspections with this tool are performed on external pipe surface only and generally does not require any graphitisation removal via grit-blasting.

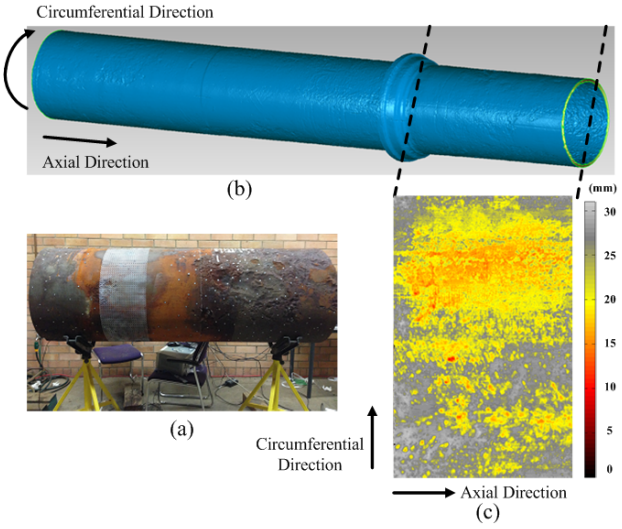

Figure 3: a) a grit-blasted pipe segment, b) the full 3D profile of a pipe section of about 5 meters long, c) The remaining wall thickness map of a pipe segment generated by processing 3D laser scanner data

3.2 Evaluation Metrics

To evaluate the performance of a model, an objective approach is to compare the prediction results against the

ground-truth using explicit numerical criteria [Hore and Ziou, 2010]. In our previous studies, given a reference thickness map $f_{M\times N}$ and a candidate thickness map $g_{M\times N}$, Root-Mean-Square Error (RMSE) as defined in equation 7 has been employed to evaluate the goodness of prediction. One of the benefits of RMSE lies in that it has the same unit as the quantity being measured. A smaller RMSE indicates smaller point-to-point discrepancy in average. The RMSE between two identical pipe wall thickness maps is zero. Another metrics adopted in this work is the Structural Similarity Index (SSIM), as shown in equation 8. SSIM is originally developed for quality assessment of gray-scale images [Wang *et al.*, 2004]. Comparing to RMSE, SSIM also takes structural information into consideration. For SSIM value of zero means no correlation between the reference and the candidate, and SSIM value of one means a perfect match [Hore and Ziou, 2010]. The motivation of introducing multiple metrics is to provide complementary information for evaluating the performance of the model.

$$RMSE(f,g) = \sqrt{\frac{1}{MN}\sum_{i=1}^{M}\sum_{j=1}^{N}(f_{ij}-g_{ij})^2} \qquad (7)$$

$$SSIM(f,g) = l(f,g)c(f,g)s(f,g) \qquad (8)$$

where l,c,s, are functions comparing luminance, contrast and structure information of the reference and the candidate. More details on SSIM can be found in literature [Hore and Ziou, 2010] [Wang *et al.*, 2004].

4 Results

4.1 Inference Results

Gaussian Processes inference results from two pipe segments S11 and S5 are presented in Figure 4 and Figure 5 in the form of test output mean. The associated variance on each point is also available. It is shown in Figure 4 that in the presence of spatially close training data, the inference result is somehow visually meaningful. The associate variances, which is not visualised here, are relatively low. However, without local training data the inference result can be much less visually meaningful as shown in the case of pipe segment S5 in Figure 5. In this experiment, Gaussian Processes modelling and inference with either covariance function gives a flat surface associate with large variance values. Even worse, in some scenarios the global location information as the input to the Gaussian Processes are not available which makes inference infeasible. Therefore instead of providing probabilistic inference results, in these situations generating realisations of a Gaussian Process model makes a better interpretation plus it also serves as an input to Monte Carlo simulation if required.

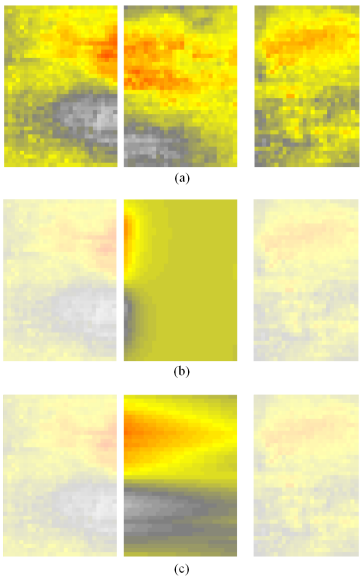

Figure 4: A comparison of inference results on pipe segment S11. (a) the ground-truth of pipe segment S10, S11 (middle) and S12. The horizontal blank spaces between thickness maps are left purposely and have the same scale as the maps to reflect the actual distances between them, and GP inference result of S11 using (b) the Matern covariance function and (c) the proposed composite covariance function

4.2 Realisation Results

Realisation results are evaluated with leave-one-out cross validation. Each time one pipe segment is kept for test and the rest eleven pipe segments are utilised in training. Then the model described by mean and covariance functions is simulated according to the dimension of the test data to generate certain number of realisations which are then compared against the ground-truth of the test data.

Table 1 shows the evaluation results using RMSE as the evaluation metric, based on the average RMSE results on ten thousand realisations in each training-realisation-comparison cycle. In 11 out of 12 cases, modelling with the proposed composite covariance function outperform the results with the Matérn covariance function. Regarding the exception, the performance gap in terms of the reported RMSM value is trivial.

Similarly, Table 2 shows the evaluation results using SSIM as the evaluation metric, based on the average SSIM results of ten thousand realisations in each training-realisation-comparison cycle. In all 12 cases modelling with the proposed composite covariance function outperform the results with the Matérn covariance function.

As typical examples, a visualisation of closest realisations on S2 and S9 is presented in Figure 6. In each

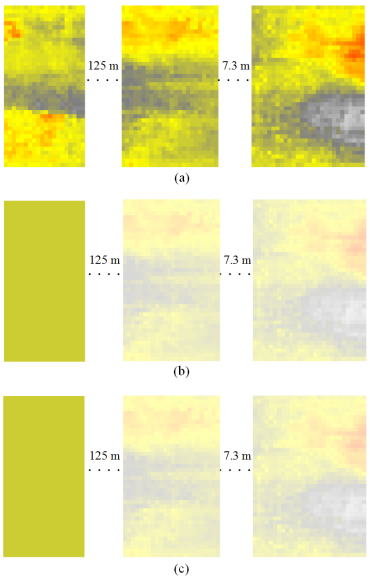

Figure 5: A comparison of inference results on pipe segment S5. (a) the ground-truth of pipe segment S5 (left), S1 and S10 and the indicated actual distances between them, and GP inference result of S5 using (b) the Matern covariance function and (c) the proposed composite covariance function

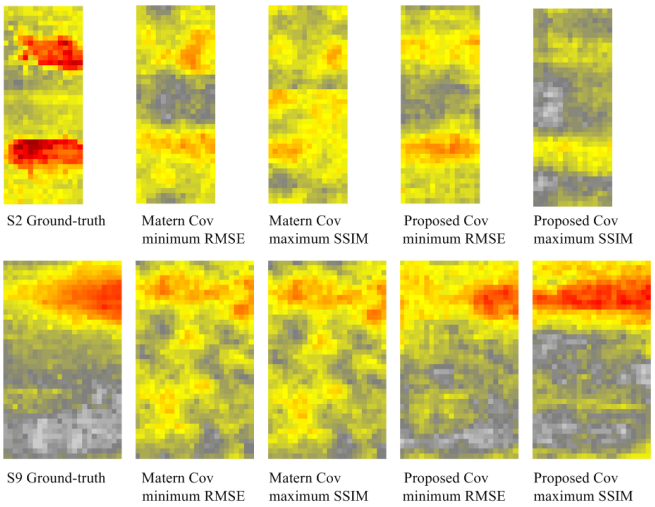

Figure 6: Comparison of the closest realisations from different covariance functions against different metrics

Table 1: Cross-validation results measured in RMSE

Test Map ID	Customised Cov Avg. RMSE (mm)	Matérn Cov Avg. RMSE (mm)
S1	2.82	3.13
S2	5.32	5.36
S3	3.26	3.04
S4	3.14	3.33
S5	2.96	3.10
S6	3.77	3.83
S7	4.07	4.48
S8	3.43	3.59
S9	4.18	4.81
S10	3.42	3.75
S11	3.54	3.89
S12	3.05	3.26
Avg.	**3.58**	**3.80**

scenario the closest realisation to the test ground-truth is selected from the corresponding ten thousand realisations. According to the results in Table 1, in terms of RMSE S2 gives the only result that is in favour of using the Matérn covariance function. This can be partially confirmed in the visualisation result. Closest realisation in SSIM using the proposed covariance function suggests that SSIM relies more on the structural similarity than point-to-point difference. On S9, closest realisations generated using the simple covariance function are identical, which means RMSE and SSIM are somehow dependent. It can also be visually justified that closest realisations generated using the proposed composite covariance function outperform their peers, which agrees with the results reported in Table 1 and Table 2.

In the real-world scenario the ground-truth data is rarely accessible, so that the closest realisation will not be able to be picked up. Therefore without a specific selection criteria all realisations will be provided for further analysis. However, if certain indication like the standard deviation or the minimum value of the thickness measurements in a realisation is set to reflect the quality of that pipe segment, best-case and worst-case scenarios can be selected from the realisation set.

5 Conclusion

This paper presents an application of Gaussian Processes to capture the spatial correlation of 2.5D pipe thickness data from local inspection outcomes, and to sample the learned model to produce predictions of the condition of the pipe in unobserved areas. Using condition assessment of buried water pipes as the specific application, we incorporate pipe properties-specific in the design of the covariance function. The proposed covariance function is an anisotropic composite kernel that models the spatial correlation of pipe wall thickness measurements. Based on the learned model, we proposed to use Gaussian Process realisations, as opposed to inference, to extrapolate the conditions of the same pipe cohort. The prediction performance is then evaluated using two different met-

Table 2: Cross-validation results measured in SSIM

Test Map ID	Customised Cov Avg. SSIM	Matérn Cov Avg. SSIM
S1	0.19	0.12
S2	0.17	0.14
S3	0.15	0.12
S4	0.19	0.13
S5	0.20	0.14
S6	0.15	0.12
S7	0.23	0.16
S8	0.23	0.19
S9	0.22	0.13
S10	0.17	0.11
S11	0.18	0.12
S12	0.19	0.13
Avg.	**0.19**	**0.13**

rics. Experimental results show that the proposed composite covariance function is capable of building a spatial correlation model for pipe wall thickness map and realisations of this model have the potential of being fed to Monte Carlo simulation for failure risk related structural analysis. Future work considers the analysis on the realisations to decide what is the most useful sample for predicting the pipe failure.

6 Acknowledgements

This publication is an outcome from the Critical Pipes Project (www.criticalpipes.com) funded by Sydney Water Corporation, Water Research Foundation of USA, Melbourne Water, Water Corporation (Western Australia), UK Water Industry Research Ltd, South Australia Water Corporation, South East Water, Hunter Water Corporation, City West Water, Monash University, University of Technology Sydney and University of Newcastle. The research partners are Monash University (lead), University of Technology Sydney and University of Newcastle.

References

[Bishop, 2006] Christopher M. Bishop. *Pattern recognition and machine learning*. Information science and statistics. Springer, New York, 2006.

[Bonds *et al.*, 2005] Richard W Bonds, Lyle M Barnard, A Michael Horton, and Gene L Oliver. Corrosion and corrosion control of iron pipe: 75 years of research. *Journal American Water Works Association*, pages 88–98, 2005.

[Davies and Bryant, 2013] Tilman M Davies and D Bryant. On circulant embedding for gaussian random fields in R. *Journal of Statistical Software*, 55(9):1–21, 2013.

[Hore and Ziou, 2010] Alain Hore and Djemel Ziou. Image quality metrics: PSNR vs. SSIM. In *20th International Conference on Pattern Recognition (ICPR)*, pages 2366–2369. IEEE, 2010.

[Kersting *et al.*, 2007] K. Kersting, C. Plagemann, P. Pfaff, and W. Burgard. Most likely heteroscedastic gaussian process regression. In *International Conference on Machine Learning (ICML)*, Corvallis, Oregon, USA, 2007.

[Kroese and Botev, 2013] Dirk P Kroese and Zdravko I Botev. Spatial process generation. In V. Schmidt, editor, *Lectures on Stochastic Geometry, Spatial Statistics and Random Fields, Volume II: Analysis, Modeling and Simulation of Complex Structures*. Springer-Verlag, 2013.

[Li and Mahmoodian, 2013] CQ Li and M Mahmoodian. Risk based service life prediction of underground cast iron pipes subjected to corrosion. *Reliability Engineering & System Safety*, 119:102–108, 2013.

[Lord *et al.*, 2014] Gabriel J. Lord, Catherine E. Powell, and Tony Shardlow. *An Introduction to Computational Stochastic PDEs*. Cambridge texts in applied mathematics. Cambridge University Press, 2014.

[Miro *et al.*, 2013] Jaime Valls Miro, Jeya Rajalingam, Teresa Vidal-Calleja, Freek de Bruijn, Roger Wood, Dammika Vitanage, Nalika Ulapane, Buddhi Wijerathna, and Daoblige Su. A live test-bed for the advancement of condition assessment and failure prediction research on critical pipes. In *Proceedings of the Leading-Edge Strategic Asset Management Conference (LESAM13)*, 2013.

[O'Callaghan and Ramos, 2012] Simon T. O'Callaghan and Fabio T. Ramos. Gaussian process occupancy maps. *International Journal of Robotics Research*, 31(1):42–62, 2012.

[Petersen *et al.*, 2014] R.B. Petersen, R.E. Melchers, et al. Long term corrosion of buried cast iron pipes in native soils. In *Proceedings of the Annual Conference of the Australasian Corrosion Association 2014: Corrosion and Prevention 2014*. Australasian Corrosion Association, 2014.

[Rajeev *et al.*, 2014] Pathmanathan Rajeev, Jayantha Kodikara, Dilan Robert, Peter Zeman, and Balvant Rajani. Factors contributing to large diameter water pipe failure. *Water Asset Management International*, 10:10, 2014.

[Rasmussen and Nickisch, 2010] Carl E. Rasmussen and Hannes Nickisch. Gaussian processes for machine learning (GPML) toolbox. *The Journal of Machine Learning Research*, 11:3011–3015, 2010.

[Rasmussen and Williams, 2006] Carl E. Rasmussen and Christopher K. I. Williams. *Gaussian Process for Machine Learning*. MA:MIT press, Cambridge, 2006.

[Schlather *et al.*, 2015] Martin Schlather, Alexander Malinowski, Peter J Menck, Marco Oesting, and Kirstin Strokorb. Analysis, simulation and prediction of multivariate random fields with package randomfields. *Journal of Statistical Software*, 63(8):1–25, 2015.

[Schneider, 2009] Charles Schneider. Application of extreme value analysis to corrosion mapping data. In *Paper presented at 4th European-American Workshop on Reliability of NDE*, volume 24, page 26, 2009.

[Skinner *et al.*, 2014] Bradley Skinner, Teresa Vidal-Calleja, Jaime Valls Miro, Freek De Bruijn, and Raphael Falque. 3d point cloud upsampling for accurate reconstruction of dense 2.5 d thickness maps. In *Australasian Conference on Robotics and Automation*, 2014.

[Smith *et al.*, 2010] Mike Smith, Ingmar Posner, and Paul Newman. Efficient non-parametric surface representations using active sampling for push broom laser data. In *Proceedings of Robotics: Science and Systems VI*, 2010.

[Spanos and Zeldin, 1998] P.D. Spanos and B.A. Zeldin. Monte carlo treatment of random fields: a broad perspective. *Applied Mechanics Reviews*, 51(3):219–237, 1998.

[Sun *et al.*, 2015] Liye Sun, Teresa Vidal-Calleja, and Jaime Valls Miro. Bayesian fusion using conditionally independent submaps for high resolution 2.5 d mapping. In *IEEE International Conference on Robotics and Automation (ICRA)*, pages 3394–3400. IEEE, 2015.

[Tartakovsky and Xiu, 2006] Daniel M. Tartakovsky and Dongbin Xiu. Stochastic analysis of transport in tubes with rough walls. *Journal of Computational Physics*, 217(1):248–259, 2006.

[Tesch *et al.*, 2011] Matthew Tesch, Jeff Schneider, and Howie Choset. Using response surfaces and expected improvement to optimize snake robot gait parameters. In *IEEE/RSJ International Conference on Intelligent Robots and Systems (IROS)*, pages 1069–1074. IEEE, 2011.

[Ulapane *et al.*, 2014] Nalika Ulapane, Alen Alempijevic, Teresa Vidal-Calleja, Jaime Valls Miro, Jeremy Rudd, and Martin Roubal. Gaussian process for interpreting pulsed eddy current signals for ferromagnetic pipe profiling. In *IEEE 9th Conference on Industrial Electronics and Applications (ICIEA)*, pages 1762–1767. IEEE, 2014.

[Vasudevan *et al.*, 2009] S. Vasudevan, F. Ramos, E. Nettleton, H. Durrant-Whyte, and A. Blair. Gaussian process modeling of large scale terrain. In *IEEE International Conference on Robotics and Automation (ICRA)*, pages 1047–1053, 2009.

[Vidal-Calleja *et al.*, 2014] Teresa Vidal-Calleja, Daobilige Su, Freek De Bruijn, and Jaime Valls Miro. Learning spatial correlations for Bayesian fusion in pipe thickness mapping. In *IEEE International Conference on Robotics and Automation (ICRA)*, pages 683–690, 2014.

[Wang *et al.*, 2004] Zhou Wang, Alan C. Bovik, Hamid R. Sheikh, and Eero P. Simoncelli. Image quality assessment: from error visibility to structural similarity. *IEEE Transactions on Image Processing*, 13(4):600–612, 2004.